Electron Transfer in the Reaction Center of the *Rb. sphaeroides* R-26 Studied by Transient Absorption

Marcin Ziolek,[†] Natalia Pawlowicz,[‡] Ryszard Naskrecki,[‡] and Andrzej Dobek*[,‡]

Center for Ultrafast Laser Spectroscopy, A. Mickiewicz University, Umultowska 85, 61-614 Poznan, Poland, and Faculty of Physics, A. Mickiewicz University, Umultowska 85, 61-614 Poznan, Poland

Received: February 8, 2005; In Final Form: July 19, 2005

Electron transfer at the reaction center of the purple photosynthetic bacterium *Rb. sphaeroides* R-26 was measured at room temperature by the time-resolved transient absorption spectroscopy technique with 200 fs temporal resolution. The absorbance changes characteristic of the excited state of the primary donor and extending over the whole spectral range investigated from 350 nm up to 720 nm appeared after excitation with a laser pulse of about 100 fs duration at 800 nm. The time evolution of the spectra reflected the excitation of bacteriochlorophylls (BChl) M and L and the subsequent transfer of this excitation to the primary electron donor (P), with the time constant shorter than 1 ps. The decay time constant of the excited primary donor P was determined as about 3 ps, and it was faster than the rise of the reduced intermediary acceptor bacteriopheophytin ($BPhe_L$). Photoreduction of $BPhe_L$ and its further reoxidation was clearly observed as an increase in its bleaching band intensity at around 540 nm in about 4 ps and its decrease in about 200 ps. Our findings support the theoretical model assuming the involvement of the intermediate state P^+BChl^- in the so-called "two-step" model. In this model an electron is transferred in a sequence from the excited special pair P^* to bacteriochlorophyll, $BChl_L$, then to bacteriopheophytin, $BPhe_L$, and further on to quinone, Q_A. The branched charge separation, partially via P and partially via $BChl_L$, was also observed.

Introduction

Photosynthetic reaction centers (RC) are pigment−protein complexes, mainly hydrophobic, in which transmembrane charge separation and stabilization processes drive all the subsequent chemistry of photosynthesis (see, for example, refs 1 and 2 for review). After light excitation of the bacterial RC the reactions start from the singlet excited state $^1P^*$ of a primary electron donor P (a dimer of bacteriochlorophylls *a*) which decays in a few picoseconds by ultrafast electron transfer to a primary electron acceptor $BPhe_L$ (bacteriopheophytin *a*), creating the primary radical pair $P^+BPhe_L^-$. Different types of measurements have shown that after the primary charge separation, the electron is transferred to a secondary electron acceptor, ubiquinone Q_A, in about 200 ± 50 ps.[3−5] When Q_A is prereduced or removed, the forward electron transfer is blocked at the level of $BPhe_L^-$ and the primary radical pair decays by charge recombination. It has been calculated that the characteristic time of charge separation must be of a few picoseconds or less. Martin et al.[6] for the first time demonstrated that in the RC of *Rb. sphaeroides* R-26, one-step charge separation takes place in 2.8 ± 0.3 ps and found no evidence for the second faster kinetics attributable to the reduction of $BChl_L$ (bacteriochlorophyll L), the intermediate accessory molecule. The opposite conclusion was drawn from the experimental study by Holtsapfel et al.[7,8] At selected wavelengths within the $\lambda = 800$ nm absorption band the biphasic kinetics was found, with time constants of 3.5 ± 0.4 and 0.9 ± 0.3 ps attributed to the creation of $BChl_L^-$ and reduction of $BPhe_L$, respectively. Another model of primary charge separation proposes that the excited bacteriochlorophyll $BChl_L^*$ acts as the primary electron donor.[9] An electron is transferred from $BChl_L^*$ to $BPhe_L$, giving $BChl_L^+BPhe_L^-$, and a subsequent charge transfer forms $P^+BChl_LBPhe_L^-Q_A$.

The features of the monomeric bacteriochlorophyll ($BChl_L$) as a real electron carrier in the *Rb. sphaeroides* RCs were further studied in the 1990s by the Zinth group[10−14] and Shuvalov group[15] through the use of subpicosecond absorption spectroscopy. In ref 10 the authors have found that for temperatures from 300 to 15 K the electron transfer to BPhe is characterized by a biphasic time dependence. The two time constants of 3.5 and 1.2 ps (at 300 K) decrease continuously with temperature. The observations have been rationalized by a two-step electron-transfer model. An additional dichroic study in the spectral range of 920−1040 nm has shown a strong dichroism of the 0.9 ps kinetic component of the transfer absorption data.[11] This dichroism is consistent with a stepwise electron transfer via the accessory bacteriochlorophyll. In another work[12] the energetics of the primary electron-transfer reaction has been measured on modified bacterial reaction centers by introducing Phe *a* (from plant). The free energy of $P^+BChl_L^-$ lies at about 450 cm^{-1} below P^* in these modified RCs, and the electron-transfer kinetics are different from those in the native samples.[13] The accessory $BChl^-$ anion can be directly observed at around 1000 nm. The data have proved that primary electron transfer involves the accessory bacteriochlorophyll as the actual electron carrier. In ref 14 the authors have reported experiments on RCs with pigments that have energetically raised the level of $P^+BChl_L^-$. The results suggest a sequential electron-transfer mechanism even for the unfavorable energetic situation and have shed light on the energetic optimization strategies in the native systems. The plant pheophytin-exchanged RCs have also been studied

* To whom correspondence should be addressed. Fax: +48-61-829-5155. E-mail: dobek@amu.edu.pl.
[†] Center for Ultrafast Laser Spectroscopy, A. Mickiewicz University.
[‡] Faculty of Physics, A. Mickiewicz University.

10.1021/jp050682i CCC: $30.25
Published on Web 08/31/2005

in low temperatures.[15] The authors have detected the spectral change at around 1020 nm, which indicated the formation of $BChl^-$ with 1.6 ps, similarly as in the native RCs. The observation identifies the accessory BChl as the primary electron acceptor. These results also support a two-step model for primary electron transfer in the native reaction centers.

Important conclusions on the involvement of $P^+BChl_L^-$ as an intermediate in *Rb. sphaeroides* R26 have been drawn from analysis of wave packet oscillation features. Spörlein et al.[16] have shown that modulated absorption features are observed throughout the whole wavelength region 920−1100 nm, when at $T = 30$ K the RCs with Q_A^- are excited by 110 fs pulses at 865 nm. The observations have been explained by the motion of the vibrational wave packet on the excited-state potential surface of the special pair P^* and its effect on stimulated emission and excited-state absorption.

The application of very short light pulses of an order of some tens of femtoseconds allowed the Shuvalov group[17−22] to investigate further the subpicosecond oscillations in the cofactor bands in RCs of *Rb. sphaeroides* R-26. Streltsov et al.[17,18] have found such oscillations in the $BChl_L$ band in native and $BChl_M$ in modified RCs at 293 K using 30 fs excitation pulses at 865 nm. The authors have concluded that the protein vibrational mode at 30 cm^{-1} is likely to play an important role in the electron transfer. The oscillations in the femtosecond kinetics of the stimulated emission from P^* in the native, $BChl_M$-modified, and mutant (YM210W) RCs have been observed at low and room temperatures.[18] The relative enhancement of the modes in 805 nm kinetics may modulate the distance between P and $BChl_L$ molecules, which could be important for electron transfer.

Yakovlev et al.[19] and Yakovlev and Shuvalov[20] have studied the formation of the nuclear wave packet on the potential energy surface of P^* induced by 30 fs of Phe modified with Q_A^- RCs. Such an excitation leads to a reversible or irreversible appearance of the $P^+BChl_L^-$ state monitored by the 1020 nm band characteristic of $BChl_L^-$. The reversible appearance of the state is characterized by two (130 and 320 cm^{-1}) vibrational modes. The irreversible formation of the $P^+B_A^-$ state with a time constant of 3 ps is accompanied by oscillations of frequencies 9 and 33 cm^{-1}. The study has been continued in ref 21 in which the authors reported on the formation and propagation of the nuclear wave packet on the potential energy surface of P^* and the charge separated states $P^+BChl_L^-$ and $P^+BPhe_L^-$ in the spectral range 720−1060 nm. In this study, the processes have been monitored by measuring coherent oscillations in kinetics of the time evolution of the stimulated emission of P^* band at 935 nm, the absorption band of $BChl_L^-$ at 1020 nm, and the bleaching band of $BPhe_L$ at 760 nm. In ref 22 the authors have shown how they had found the nuclear wave packet motions on the potential energy surface of the excited state of P^* and how it leads to a coherent formation of the charge separated states: $P^+BChl_L^-$, $P^+BPhe_L^-$, and $P^+BPhe_M^-$ in the native, pheophytin-modified, and mutant RCs of *Rb. sphaeroides* R-26.

Recently, a new pathway of charge separation in the monomeric bacteriochlorophyll has been experimentally observed.[23−25] In ref 24 the authors have performed femtosecond pump−probe experiments at 77 K on the wild-type reaction centers of *Rb. sphaeroides*. They have selectively excited P or $BChl_L$ at 880 or 796 nm, respectively, and in both cases the formation of $P^+H_A^-$ was associated with similar time constants of 1.5 and 1.7 ps. Global analysis has shown that a mixture of $P^+BChl_L^-$ and P^* is formed in parallel from $BChl_L^*$ on a subpicosecond time scale. In ref 25 van Brederode and van Grondelle have demonstrated the existence of multiple ultrafast routes for charge separation in bacterial RCs. The experiments discussed suggest that a "special" pair is not an absolute requirement for an ultrafast electron transfer in RCs. The charge separation can be driven directly by the excited state of accessory monomeric $BChl_L$. The role of the accessory monomeric chlorophyll acting as primary electron donor has been also suggested in the photosystem II RC[25,26] and considered in the reaction pathways in photosystem I.[27]

In the present paper we report a study of changes in the absorbance of the RC of *Rb. sphaeroides* R-26 in the range of 350−715 nm measured at room temperature. They are associated with the electron transfer at the reaction center, and the rate constant of this transfer is measured with a 200 fs time resolution. Direct excitation of the Q_y absorption band of $BChl_L$ and $BChl_M$ at $\lambda = 800$ nm permitted a study of absorption bands far from this wavelength.

Materials and Methods

Isolated reaction centers were resuspended in 5 μM RCs in 10 mL of 10 mM Tris, pH 8.0, 0.1% LDAO, and 0.1 mM Na-ascorbate. RC suspension continuously flowed through the sample cell at a rate that enabled the total exchange of the excited volume for each laser shot. The sample cell (laboratory made) with the windows of fused silica plates had an absorption layer of 2 mm in thickness.

The setup used for the transient absorption measurements was described in detail earlier.[28] The output of the femtosecond laser system (Ti:Sapphire, Spectra Physics) was set at 100 Hz repetition rate providing light pulses with time duration between 80 and 120 fs (full width at half maximum, fwhm) at $\lambda = 800$ nm with the 15 nm spectral bandwidth. The pump−pulse energy was 35 μJ; the probe pulse had less than 1 μJ energy covering a spectral range between 330 and 730 nm. Such white light continuum pulses were generated in a 2 mm thick calcium fluoride plate. To avoid the temperature effects this plate was rotated at a frequency of a few Hertz. The pump was directed through a fixed optical path and was focused inside the sample cell. To reduce the photodegradation of the liquid sample, a continuous flow through the excited volume at a rate up to 50 mL/min was used, enabling the total exchange of the excited volume in 10 ms. All the connections in the circulation system were made with Teflon tubing. The probe beam passed through an optical delay line consisting of a retroreflector (hollow corner cube) mounted on a computer controlled motorized translation stage and then it was converted to white light continuum pulses whose diameter was 2−5 times smaller than that of the pump. Both beams (pump and probe) intersected at an angle of 2° and spatially overlapped into a flowing sample cell with fused silica windows. The spot size of the pump beam (important to know the pump power density) and the alignment of the spatial pump−probe overlap were controlled at the entrance window of the sample cell by a Spiricon visualization system including a small CCD camera and a long focal objective. A much magnified cross-section of the probe and pump beams was sent to a computer to determine the diameters of these beams as fwhm, to an accuracy better than 5%.

A grating polichromator (Spectra Pro 150, Acton Research Corp.) was used in conjunction with a thermoelectrically cooled CCD camera (Back Illumin., Princeton Instr.) to record the transient spectra. The polichromator was equipped with two replaceable gratings (300 or 150 grooves/mm) giving the spectral windows of 240 and 480 nm spectral width, respectively, and setting the spectral resolution at 0.47 and 0.94 nm/pixel,

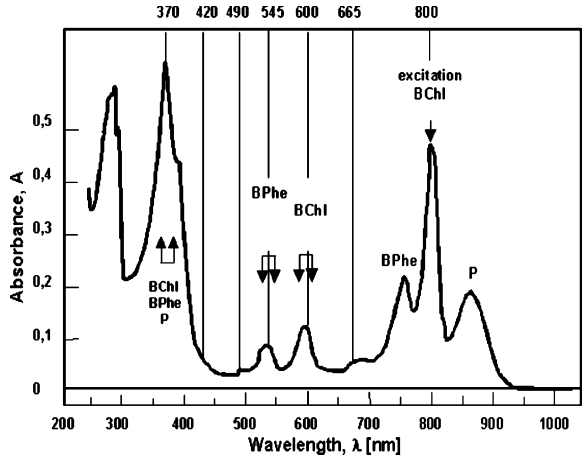

Figure 1. Absorption spectrum of photosynthetic purple bacteria *Rb. sphaeroides* reaction centers. The excitation and transient absorption wavelengths are indicated.

respectively. It should be noted that this theoretical spectral resolution is affected by the accuracy of the wavelength calibration procedure and the actual resolution is equal to 1 and 2 nm/pixel, respectively. The total time window of the experiment and the smallest time step of the transient spectra measurements were determined by the optical delay line and were 1.2 ns and 3.3 fs, respectively.

To improve the signal-to-noise ratio, the transient absorption measurements were performed in two-beam geometry (probe and reference) with two synchronized choppers in the pump and probe paths, respectively, which allowed substantial elimination of the influence of the laser beam fluctuations and, consequently, measurements of much lower values of the small optical density changes. The data (full transient spectrum) were collected during a fixed integration time set to 96 ms (average over 9 laser pulses). In such an experimental setup, the optical density changes (ΔOD) can be measured to an accuracy of $\sim$0.0005 in the 330−730 nm spectral range. The measurements were performed at the magic angle of 54.7° between the polarization of the pump and probe beam.

All the spectra analyzed were corrected for group velocity dispersion effect according to the standard numerical scheme.[29] The chirp of white light continuum was obtained by measuring two-photon absorption in a very thin (150 μm) BK7 glass plate (pumping with a second harmonic of 800 nm pulses). An additional contribution of dispersion, due to the front window of the sample cell, was calculated from the Sellmeier equation. Trace analysis was based on the fit of the convolution of the instrumental function (pump−probe cross-correlation function) with a three-exponential function. The fwhm of the pump−probe cross-correlation function was about 200 fs. It was determined by the measurements of the stimulated Raman amplification signal (narrow band at around 635 nm)[30] in water in the same sample cell and the same excitation wavelength as used for the reaction centers measurements. The pump−probe cross-correlation function was temporally broadened with increasing difference between pump and probe wavelength due to the group velocity dispersion in the sample.[31] No transient absorption signal from the pure buffer (without reaction centers) was observed except for the above-mentioned stimulated Raman amplification from water.

Results and Discussion

Figure 1 shows the ground-state absorption spectrum of photosynthetic purple bacteria *Rb. sphaeroides* RCs. The excitation and transient absorption wavelengths tested are indicated. The figure shows the main absorption bands and their assignment to the components of the photosynthetic membrane.

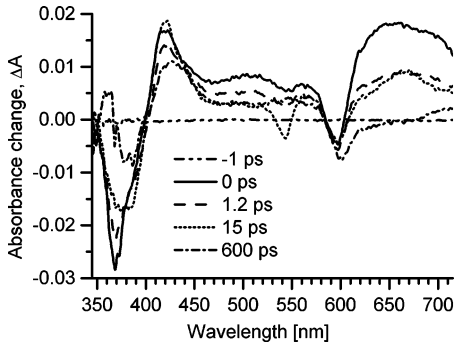

Figure 2. Absorbance changes observed in *Rb. sphaeroides* R-26 reaction centers at various delay times.

Figure 2 shows the absorbance changes measured in the spectral region studied, from $\lambda = 350$ nm to $\lambda = 715$ nm. The exemplary delay times between the probe and the excitation pulse at $\lambda = 800$ nm were chosen as −1, 0, 1.2, 15, and 600 ps. The trace marked with −1 ps corresponds to the signal obtained before the pump−probe temporal overlap. The difference spectra at these time intervals can be assigned to P^*, P^+, $BChl_M^*$, $BChl_L^*$, $BChl_L^-$, $BPhe_L^-$, and Q_A^-. The time evolution of the spectra reflects the excitation of bacteriochlorophylls M and L and the subsequent transfer of this excitation to the primary electron donor, $BChl_{M,L}P + h\nu \rightarrow BChl_{M,L}^*P \rightarrow BChl_{M,L}P^*$. In the spectra shown in Figure 2 the electron-transfer reactions $P^*BChl_L \rightarrow P^+BChl_L^-BPhe_L \rightarrow P^+BChl_LBPhe_L^-Q_A \rightarrow P^+BChl_LBPhe_LQ_A^-$ are also reflected.

To analyze the rates of these reactions, the absorption changes ΔA_{fit} were fitted with a constant plus three exponentials (convoluted with the instrumental function)

$$\Delta A_{fit} = A_0 + A_1 \exp(-t/\tau_1) + A_f \exp(-t/\tau_f) + A_s \exp(-t/\tau_s), \quad (1)$$

where t is the time after excitation.

Just after excitation, within the time of the pump−probe cross-correlation function (fwhm = 200 fs), two bands of transient absorption appear at $\lambda = 400-580$ nm (with maximum at $\lambda = 420$ nm) and at $\lambda = 610-715$ nm. Also two bands of negative transient absorption (depopulation) appear within this time, one at $\lambda = 350-400$ nm and the other at $\lambda = 580-610$ nm. Both depopulation bands coincide with the position of the steady-state absorption bands of the chlorophyll.

For times shorter than 1.2 ps, after excitation, a very fast decay (<500 fs) of most of the bands is observed. The simplest interpretation of this decay is the transfer of the excitation from BChl to P with the τ_1 time constant. However, the data obtained may also suggest a branched charge separation, partially via P and partially via BChl. In the region above 600 nm, where the predominant contribution comes from excited BChl, the amplitude of the signal decreases about two times between 0 and 1.2 ps after excitation, while the bleaching signal in the 570−600 nm region (originating from BChl depopulation, see Figure 1) remains nearly constant (see Figure 2). This may suggest that the excited BChl for a large fraction decays into $P^+BChl_L^-$, without intermediate P^*. This finding is in agreement with the recent results[23−25] derived from the analysis of the measurements in the spectral region above 700 nm. On the other hand, in our case the constant value of the bleaching signal may originate from the interplay of the decay of the positive transient

TABLE 1: Results of the Two-Exponential Fit in Given Spectral Ranges

spectral range (nm)	τ_f (ps)	τ_s (ps)
380−400	(−)[a] 5.6 ± 1.6	(+)[a] 185 ± 33
410−435	(+) 5.0 ± 0.6	(−) 216 ± 26
455−525	(−) 3.1 ± 0.5	
525−550	(−) 4.0 ± 0.7	(+) 231 ± 48
615−635	(−) 4.8 ± 2.3	(−) 211 ± 16
655−680	(+) 6.8 ± 1.3	(−) 208 ± 8

[a] The signs (−) or (+) indicate that the absorbance changes connected with the component are negative (decrease in transient absorption or increase in depopulation) or positive (the opposite), respectively.

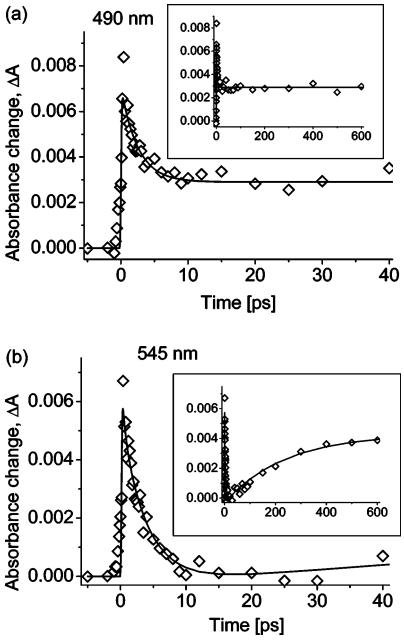

Figure 3. Kinetics of absorbance changes at 490 nm (a) and 545 nm (b) for the reaction centers from *Rb. sphaeroides* R26 in a 40 ps time window (and in a 600 ps time window shown as inset). The smooth curves represent the convolution of the pump−probe cross-correlation function with eq 1. The best fit to the observed kinetics is obtained for the following parameters: (a) 490 nm, $A_0 = 0.003 \pm 0.001$, $A_1 = 0$, $A_f = 0.004 \pm 0.001$, $\tau_f = 2.5 \pm 1.2$ ps, $A_s = 0$; (b) 545 nm, $A_0 = 0.004 \pm 0.001$, $A_1 = 0.0008 \pm 0.0002$, $\tau_1 = 0.48 \pm 0.18$ ps, $A_f = 0.005 \pm 0.001$, $\tau_f = 3.9 \pm 1.5$ ps, $A_s = -0.005 \pm 0.001$, $\tau_s = 236 \pm 99$ ps.

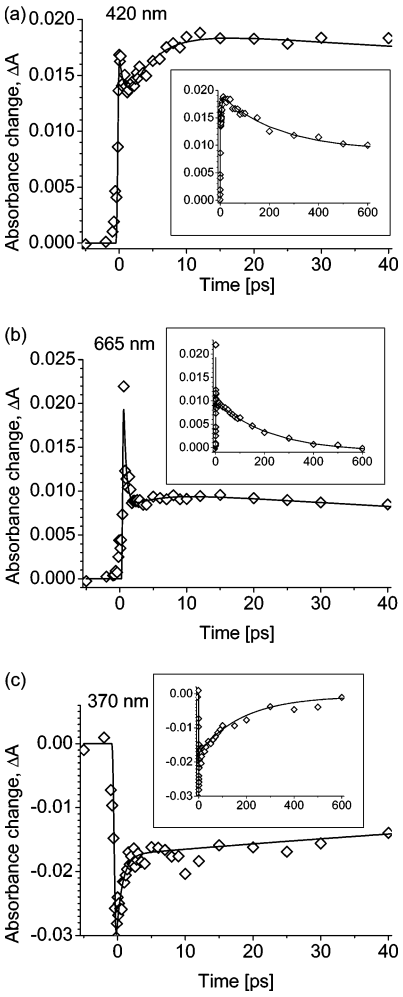

Figure 4. Kinetics of absorbance changes at 420 nm (a), 665 nm (b), and 370 nm (c) for the reaction centers from *Rb. sphaeroides* R-26 in a 40 ps time window (and in a 600 ps time window shown as inset). The smooth curves represent the convolution of the pump−probe cross-correlation function with eq 1. The best fit to the observed kinetics is obtained for the following parameters: (a) 420 nm, $A_0 = 0.009 \pm 0.001$, $A_1 = 0.005 \pm 0.002$, $\tau_1 = 0.78 \pm 0.52$ ps, $A_f = -0.008 \pm 0.004$, $\tau_f = 4.2 \pm 1.5$ ps, $A_s = 0.010 \pm 0.001$, $\tau_s = 235 \pm 80$ ps; (b) 665 nm, $A_0 = -0.001 \pm 0.001$, $A_1 = 0.012 \pm 0.005$, $\tau_1 = 0.4 \pm 0.3$ ps, $A_f = -0.002 \pm 0.001$, $\tau_f = 4.4 \pm 3.1$ ps, $A_s = 0.011 \pm 0.002$, $\tau_s = 215 \pm 96$ ps; (c) 370 nm, $A_0 = 0.001 \pm 0.001$, $A_1 = -0.013 \pm 0.004$, $\tau_1 = 0.9 \pm 0.3$ ps, $A_f = 0$, $A_s = -0.017 \pm 0.003$, $\tau_s = 185 \pm 60$ ps.

absorption signal and the decay of the negative ground-state depopulation signal which overlap in the same spectral region. Thus, the quantitative analysis of this mechanism is rather uncertain, and the efficiency of this second charge separation path is difficult to evaluate.

To analyze the rates of the reactions after these ultrafast processes, the absorption changes are fitted with a constant plus only two exponentials (without τ_1 time constant) in the time range from 1.2 ps to 1 ns. The results are summarized in Table 1.

The negative absorbance changes connected with each component (each time constant) indicate that there is a decrease in the transient absorption amplitude or an increase in the depopulation amplitude, whereas the positive absorbance changes mean an increase in the transient absorption signal or a decrease in the depopulation signal with the corresponding time constant. The time constants are averaged over the fit results performed every 2 nm in given spectral ranges. The examples of kinetic traces together with the best fits at selected wavelengths are given in Figures 3 and 4. It should be noted that the averaged values of the time constants in Table 1 are much more precise than those from the fits at a particular exemplary wavelength, presented in Figures 3 and 4, and the former should rather be regarded as representative.

The time constant of the faster component, τ_f, is significantly changed in different spectral ranges, and thus, we assume that it is composed of two time constants, τ_2 and τ_3. The τ_2 time constant describes the charge separation for the $P^* \rightarrow P^+BChl_L^-$ reaction, and τ_3 is the time constant of the electron transfer from $BChl_L^-$ to $BPhe_L$. The slow component of the time constant τ_s describes the electron transfer from $BPhe_L^-$ to Q_A. The time constant τ_s agrees with the literature value of about 200 ± 50 ps.[3−5]

The results obtained support the two-step model of electron transfer from P^* to $BPhe_L$ through the intermediacy of $BChl_L$. For $\lambda = 455-525$, the observed decay, with $\tau_f = 3.1 \pm 0.5$ ps time constant, is directly related to the decay of P^* (see, for example, the kinetic at $\lambda = 490$ nm, Figure 3a). A contribution of $BPhe_L$ in this short component is excluded because there is no slow component originating from reduced bacteriopheophytin. In the other spectral ranges, where the slow component τ_s

attributed to $BPhe_L^-$ is observed, the time constant of the fast component τ_f is longer. For example, at $\lambda = 545$ nm first an increase (in $\tau_f = 3.9 \pm 1.5$ ps) and then a decrease (in $\tau_s = 236 \pm 99$ ps) in the depopulation of $BPhe_L^-$ is visible; see Figure 3b. A similar situation occurs at $\lambda = 420$ nm, where an increase (in $\tau_f = 4.2 \pm 1.5$ ps) followed by a decrease (in $\tau_s = 235 \pm 80$ ps) in the transient absorption of $BPhe_L^-$ is observed, see Figure 4a, and at $\lambda = 665$ nm ($\tau_f = 4.4 \pm 3.1$ ps, $\tau_s = 215 \pm 96$ ps); see Figure 4b.

This means that the decay of the excited primary donor P^* is faster than the rise of the reduced intermediary acceptor $BPhe_L^-$. This effect can be explained by assuming the involvement of an intermediary acceptor, bacteriochlorophyll L ($BChl_L$), in line with many recent papers mentioned in the Introduction. After the authors of refs 7 and 8 and later papers,[10−15] we assume that a charge separation $P^* \rightarrow P^+BChl_L^-$ occurs in $\tau_2 = 3.5 \pm 0.4$ ps followed by the subsequent electron-transfer $P^+BChl_L^-BPhe_L \rightarrow P^+BChl_LBPhe_L^-$ in $\tau_3 = 0.9 \pm 0.3$ ps. When the values of these time constants are taken into account, the calculations show that the increase in the reduced pheophytin occurs in a resultant value of 4.3 ps. In the study performed the appearance of $BChl_L^-$ cannot be measured directly because its maximal transient concentration is very small (about 16% of the maximal transient concentration of P^*). In addition, for some bands the signal originating from $BPhe_L^-$ overlaps the signal of P^* decay. In such cases, the fitted time constant takes an intermediate value between the decay time of P^* and the rise time of $BPhe_L^-$. It is visible, for example, for the depopulation band at $\lambda = 545$ nm, see Figure 3b, which adjoins the spectral range at $\lambda = 455-525$ nm attributed to P^*. Moreover, the kinetics may be also influenced by the second path of charge separation via the excited monomer BChl and without P, resulting in the overall time constant τ_f being faster than $\tau_2 = 3.5$ ps. The intermediate state, P^+BChl^-, is also considered in the "super-exchange" model,[32] in which the electron immediately travels to $BPhe_L$, and $BChl_L$ functions as a virtual electron conductor. However, because of the absorption changes observed in the spectral range at $\lambda = 455-525$ nm, this model can be excluded.

The main argument for the two steps of charge separation between P and $BPhe_L$ is a shorter time of the fast component in the spectral range $\lambda = 455-525$ nm, in which no slow component is detected. In the other ranges the opposite is the case: the short component is longer and the slow component is clearly visible. An additional argument for biphasic electron transfer from the primary donor to pheophytin L comes from singular value decomposition analysis. The analysis was performed in the entire spectral range from 1.2 to 1000 ps. The number of singular values, which differ from the noise, is equal to the number of transient species participating in the spectral changes.[33,34] For the measurements discussed the following values were obtained: 1.252, 0.263, 0.134, 0.044, 0.038, 0.036, 0.034, 0.031, 0.029, 0.028, 0.027, and so on. The first four numbers can be indicated as independent of the noise values, and they point out the transient species: P^*, $BChl_L^-$, $BPhe_L^-$, and Q_A^-. It should be noted that a particular singular value does not correspond directly to a particular transient, but the contributions of all transients are linearly combined in each singular value.

We have also calculated decay-associated spectra from global fitting, accounting for the deconvolution of the recorded signals from the 1.2 to 30 ps time range with instrument response function using the written software ASUFIT from Arizona State University.[35] This was performed to obtain yet another confirmation of the presence of the two steps of charge separation between P and $BPhe_L$. Indeed, in the 525−555 nm region (in which pheophytin L certainly brings a contribution) the two-exponential fit (with the fitted time constants 3.7 and 1.0 ps) gives more than a 10% better χ^2 value than assuming the one-exponential fit (with the fitted time constant 3.6 ps). On the other hand, in the spectral region 455−525 nm (without pheophytin contribution) only one-exponential kinetics with the time constant of 2.3 ps has been fitted (under the two-exponential model the two time constants had the same value).

The negative signal observed at $\lambda < 400$ nm results from the depopulation of P^+ and can be explained by the existence of the steady-state absorption of the bacteriochlorophylls. Figure 4c shows the absorbance changes observed at $\lambda = 370$ nm. Analysis of the $P^+Q_A^-$ spectrum shows that it does not change for times longer than 600 ps. The weak transient absorption band at $\lambda = 360-370$ nm and at $\lambda > 680$ nm (see Figure 2) can be related to the appearance of the transient absorption of semiquinone Q_A^-.

Recently, we have reported on our preliminary transient absorption studies of *Rb. sphaeroides* R-26 in the spectral range from 400 to 680 nm.[36] In the above paper the wavelength dependence of the fast component (from 6 to 2 ps in the 415−450 nm range) was established. However, this result was not confirmed in our present studies, and the τ_f time constant, within experimental error, did not change its value in this spectral range (see Table 1). The possible reason for such a discrepancy is a much worse signal-to-noise ratio and insufficient temporal resolution of data points collected in our previous studies (for example, compare Figure 4a from this paper to Figure 7 from ref 36). Indeed, when we performed the fitting procedure for the earlier data once again, we found that the same quality of the fit could be obtained when the amplitude of the ultrafast component τ_1 (of the fixed value 200 fs) would be increased instead of decreasing the τ_f value.

We have also tried to improve our present signal-to-noise ratio by increasing the pump−pulse energy (up to 100 μJ) and laser repetition rate (up to 1 kHz instead of 100 Hz). However, in that case we observed changes in the transient absorption spectra and their temporal evolution. The spectrum just after excitation was similar, but the amplitude of the majority of the transient absorption and depopulation bands decreased biexponentially with time constants of 1.5 ± 0.5 and 15 ± 5 ps. Moreover, the amplitude of the bleaching band of the bacteriopheophytin around 545 nm was much smaller than that in the presented data (Figure 2). A probable explanation of such a behavior is the saturation of the reaction centers by a too high pulse energy or a not high enough flow rate (that disabled the total exchange of the excited volume for each laser shot). Thus, the electron-transfer path is blocked, and other deactivation channels have to be considered. Such distortions in the temporal shape of the R-26 transients were observed, for example, in ref 37, where an additional longer component in the femtosecond regime near 800 nm was observed under saturation conditions.

The main findings of our paper are consistent with the results of the paper of van Stokkum et al.[38] in the complementary spectral range. They have studied the role of $BChl_L$ in the primary electron-transfer reaction and the complexity of the decay of the P^* state. The authors used time-resolved absorption difference spectroscopy in the range 690−1060 nm to study quinine-reduced membrane-bound wild-type *Rb. sphaeroides* RCs in order to resolve the optical changes associated with the first step of the electron-transfer process. Using global analysis of their data, the authors have obtained five lifetimes at 0.18,

1.9, 5.1, and 22 ps and a long-lived component from the processes that underline the spectral evolution of the system. This observation led them to the conclusion that the primary electron transfer is best described by a model in which the electron is passed from P^* to $BPhe_L$ via $BChl_L$, with the formation of the radical pair state $P^+BChl_L^-$. A model assuming partial direct charge separation from excited BChl was also consistent with their data.

Conclusions

The electron transfer at the reaction center of the purple photosynthetic bacterium *Rb. sphaeroides* R-26 was measured by use of the time-resolved transient absorption spectroscopy technique in the spectral range from 350 up to 720 nm on excitation with a laser pulse of about 100 fs duration at 800 nm, in the temporal range up to 1 ns. The time constant of the decay of the excited primary donor (about 3 ps) was faster than the rise of the reduced intermediary acceptor bacteriopheophytin (>4 ps). The reoxidation of bacteriopheophytin and electron transfer to quinone occurred with a time constant of about 200 ps. Our findings support the theoretical model assuming the involvement of the intermediate state P^+BChl^- in the so-called "two-step" model. In this model, an electron is transferred in a sequence from the excited special pair to bacteriochlorophyll, then to bacteriopheophytin, and further on to quinone. The branched charge separation, partially via P and partially via $BChl_L$, was also observed.

Acknowledgment. The transient absorption measurements were performed at the Center for Ultrafast Laser Spectroscopy, Adam Mickiewicz University, Poznan, Poland. The authors thank K. Gibasiewicz and J. Zmudzinski for helpful discussions and numerical calculations of the decay-associated spectra from global fitting.

References and Notes

(1) Hoff, A. J.; Deisenhofer, J. *Phys. Rep.* **1997**, *287*, 1−247.
(2) Vos, M. H.; Martin, J.-L. *Biochim. Biophys. Acta* **1999**, *1411*, 1−20.
(3) Kirmaier, C.; Holten, D. *Photosynth. Res.* **1987**, *13*, 225−260.
(4) Dobek, A.; Deprez, J.; Paillotin, G.; Leibl, W.; Trissl, H.-W.; Breton, J. *Biochim. Biophys. Acta* **1990**, *1015*, 313−321.
(5) Dressler, K.; Umlauf, E.; Schmidt, S.; Hamm, P.; Zinth, W.; Buchman, S.; Michel, H. *Chem. Phys. Lett*. **1991**, *183*, 270−276.
(6) Martin, J.-L.; Breton, J.; Hoff, A. J.; Migus, A.; Antonetti, A. *Proc. Natl. Acad. Sci. U.S.A.* **1986**, *83*, 957−961.
(7) Holtzapfel, W.; Finkele, U.; Kaiser, W.; Oesterhelt, D.; Scheer, H.; Stilz, H. U.; Zinth, W. *Chem. Phys. Lett.* **1989**, *160*, 1−7.
(8) Holtzapfel, W.; Finkele, U.; Kaiser, W.; Oesterhelt, D.; Scheer, H.; Stilz, H. U.; Zinth, W. *Proc. Natl. Acad. Sci. U.S.A.* **1990**, *87*, 5168−5172.
(9) Fischer, S. F.; Scherer, P. O. J. *Chem. Phys.* **1987**, *115*, 151−158.
(10) Lauterwasser, C.; Finkele, U.; Scheer, H.; Zinth, W. *Chem. Phys. Lett.* **1991**, *183*, 471−477.
(11) Arlt, T.; Schmidt, S.; Kaiser, W.; Lauterwasser, C.; Meyer, M.; Scheer, H.; Zinth, W. *Proc. Natl. Acad. Sci. U.S.A.* **1993**, *90*, 11757−11761.
(12) Schmidt, S.; Arlt, T.; Hamm, P.; Huber, H.; Nagele, T.; Wachtveitl, J.; Meyer, M.; Scheer, H.; Zinth, W. *Chem. Phys. Lett.* **1994**, *223*, 116−120.
(13) Schmidt, S.; Arlt, T.; Hamm, P.; Huber, H.; Nagele, T.; Wachtveitl, J.; Zinth, W.; Meyer, M.; Scheer, H. *Spectrochim. Acta, Part A* **1995**, *51*, 1565−1578.
(14) Sporlein, S.; Zinth, W.; Meyer, M.; Scheer, H.; Wachtveitl, J. *Chem. Phys. Lett.* **2000**, *322*, 454−464.
(15) Kennis, J. T. M.; Shkuropatov, A.Ya.; van Stokkum, I. H. M.; Gast, P.; Hoff, A. J.; Shuvalov, V. A.; Aartsma, T. J. *Biochemistry* **1997**, *36*, 16231−16238.
(16) Sporlein, S.; Zinth, W.; Wachtveitl, J. *J. Phys. Chem. B* **1998**, *102*, 7492−7496.
(17) Streltsov, A. M.; Aartsma, T. J.; Hoff, A. J.; Shuvalov, V. A. *Chem. Phys. Lett.* **1997**, *266*, 347−352.
(18) Streltsov, A. M.; Vulto, S. I. E.; Shkuropatov, A.Ya.; Hoff, A. J.; Aartsma, T. J.; Shuvalov, V. A. *J. Phys. Chem. B* **1998**, *102*, 7293−7298.
(19) Yakovlev, A. G.; Shkuropatov, A. Ya.; Shuvalov, V. A. *FEBS Lett.* **2000**, *466*, 209−212.
(20) Yakovlev, A. G.; Shuvalov, V. A. *J. Chin. Chem. Soc.* **2000**, *47*, 709−714.
(21) Yakovlev, A. G.; Shkuropatov, A. Ya; Shuvalov, V. A. *Biochemistry* **2002**, *41*, 2667−2674.
(22) Shuvalov, V. A.; Yakovlev, A. G. *FEBS Lett.* **2003**, *540*, 26−34.
(23) van Brederode, M. E.; Jones, M. R.; van Mourik, F.; van Stokkum, I. H. M.; van Grondelle, R. *Biochemistry* **1997**, *36*, 6855−6861.
(24) van Brederode, M. E.; van Mourik, F.; van Stokkum, I. H. M.; Jones, M. R.; van Grondelle, R. *Proc. Natl. Acad. Sci. U.S.A.* **1999**, *96*, 2054−2059.
(25) van Brederode, M. E.; van Grondelle, R. *FEBS Lett.* **1999**, *455*, 1−7.
(26) Prokhorenko, V. I.; Holzwarth, A. R. *J. Phys. Chem. B* **2000**, *104*, 11563−11578.
(27) Müller, M. G.; Niklas, J.; Lubitz, W.; Holzwarth, A. R. *Biophys. J.* **2003**, *85*, 3899−3922.
(28) Maciejewski, A.; Naskrecki, R.; Lorenc, M.; Ziolek, M.; Karolczak, J.; Kubicki, J.; Matysiak, M.; Szymanski, M. *J. Mol. Struct*. **2000**, *555*, 1−13.
(29) Nakayama, T.; Amijima, Y.; Ibuki, K.; Hamanoue, K. *Rev. Sci. Instrum*. **1997**, *68*, 4364−4371.
(30) Lorenc, M.; Ziolek, M.; Naskrecki, R.; Karolczak, J.; Kubicki, J.; Maciejewski, A. *Appl. Phys. B* **2002**, *74*, 19−27.
(31) Ziolek, M.; Lorenc, M.; Naskrecki, R. *Appl. Phys. B* **2001**, *72*, 843−847.
(32) Bixon, M.; Jortner, J.; Michel-Beyerle, M. E. *Biochim. Biophys. Acta* **1991**, *1056*, 301−315.
(33) Chen, W. G.; Braiman, M. S. *Photochem. Photobiol.* **1991**, *54*, 905−910.
(34) Yamaguchi, S.; Hamaguchi, H. *Chem. Phys. Lett.* **1998**, *287*, 694−700.
(35) ASUFIT program available at www.public.asu.edu/∼laserweb/asufit/asufit.html.
(36) Gibasiewicz, K.; Naskrecki, R.; Ziolek, M.; Lorenc, M.; Karolczak, J.; Kubicki, J.; Goc, J.; Miyake, J.; Dobek, A. *J. Fluoresc.* **2001**, *11*, 37−44.
(37) Jonas, D. M.; Lang, M. J.; Nagasawa, Y.; Joo, T.; Fleming, G. R. *J. Phys. Chem*. **1996**, *100*, 12660−12673.
(38) van Stokkum, I. H. M.; Beekman, L. M. P.; Jones, M. R.; van Brederode, M. E.; van Grondelle, R. *Biochemistry* **1997**, *36*, 11360−11368.